The MEF revisited: Low k_1 Effects versus Mask Topography Effects

Christophe Pierrat, Fortis Systems, Inc., 2061 Rockhurst Court, Santa Clara, CA 95051,
Alfred Wong, University of Hong-Kong, Pokfulam Road, Hong Kong

Abstract
At 4X magnification and k_1 approaching 0.25, primary mask features that will ultimately print on the wafer can be on the order of the wavelength for conventional exposure tool and could fall below wavelength for immersion lithography. At the same time, the aspect ratio of the features defined on the mask increases since the absorber thickness did not scale with the technology nodes. For alternating phase-shifting masks, the etch depth into the quartz required to create a 180 degree phase-shift has not scaled with technology nodes since it is proportional to the wavelength of exposure which has not scaled with technology nodes. Near wavelength and high aspect ratio mask features increase the importance of mask topography effects. Simulations can be used as a mean to de-correlate the contributions of low k_1 effects versus mask topography effects. The "thin-mask" approximation results can be compared to the "thick-mask" simulation results. The effect of the feature aspect ratio can be investigated by changing the magnification factor. The results indicated in this paper show that mask topography effects can represent a significant part of the MEEF even for binary masks.

Keywords: lithography, simulation, mask topography, diffraction, phase-shifting mask.

1 Introduction

The acceleration of the technology roadmap and the delay of replacement options have forced lithographers to extend the life of existing equipment. The delay of 157nm lithography tools is affecting the development work done on 65nm design rules making 193nm lithography a good replacement option. Using 193nm lithography to print 65nm node devices would represent the most challenging task ever undertaken by optical lithographers with a k_1 value approaching 0.3 (assuming NA=0.85, resolution = half pitch = 70nm, ITRS 2001 roadmap, year 2006). Although this value is above the minimum theoretical limit of 0.25 required to print an image, the mask feature sizes will be on the order of the wavelength of light if a 4X reduction ratio is kept for the exposure tools. The ITRS 2001 roadmap calls for 180nm minimum mask dimensions in 2005 for 80nm technology.
An additional implication for alternating phase-shifting masks is that the aspect ratio of the trench created in the quartz substrate will be on the order of 1 and in most cases well above 1 as the thickness of the chrome is on the order of 70nm and the trench depth on the order of the wavelength. With mask dimensions decreasing beyond the wavelength, mask topography effects are becoming significant. In particular, slight variations in the mask dimension will cause large changes in the transmission, resulting in disproportional changes in the printed image. This effect should be distinguished from the low-k_1 imaging effect that has come to be known as the mask error factor.
In this paper, we will review the implications of mask dimensions in the order of the exposure wavelength using rigorous simulations of the mask diffraction effects. Data was collected for binary and alternating phase-shifting masks. A comparison of various exposure tool magnifications was also used to quantify the effects.

2 Mask Feature Dimension and Aspect Ratio

2.1 Sub-wavelength mask features?

The ultimate printing challenge for optical lithography is the transfer of dense equal lines and spaces features. The resolution of current exposure systems, defined as the half-pitch of a dense lines and spaces pattern, can be derived from the Rayleigh equation and is given by:

$$CD_{wafer} = 0.25\lambda / NA$$

λ is the wavelength of the exposure tool and NA is the numerical aperture of the projection lens.
Today's conventional exposure systems use a 4X reduction where the wafer feature sizes are four times smaller than the corresponding mask feature sizes. If we make the assumption the 4X ratio will be maintained for future exposure tool generations, which so far seems to be the case, the previous equation becomes:

$$CD_{mask} = \lambda / NA$$

CD_{mask} represents the dimension on the mask of a primary feature that will ultimately print on the wafer. The case of sub-resolution features (which would not lead to a printed feature on the wafer) will not be covered in this paper.
The numerical aperture of conventional exposure tool has been steadily increasing over the past decade and is now reaching 0.85 for tools needed for the 65nm node at 193nm wavelength. The expectation is to reach NAs of 0.9 and larger in the next few years with an absolute physical limit of 1 when the exposure is performed in the air.
If the current 4X reduction ratio is maintained, the previous equation shows that primary mask features (defined as features that will ultimately print an image on the wafer) will be on the order of the wavelength. In the case of immersion lithography where NAs can reach numbers larger than 1, the primary mask features could even fall below the exposure wavelength. For an NA of 1.25, the primary mask feature dimension could reach 0.8 times the wavelength!
If we account for more stringent design requirements and OPC, the mask dimensions corresponding to primary features transferred on the wafer could even be smaller.
This observation of near or sub wavelength mask feature can be derived from the ITRS Roadmap as shown in Figure 1. The extension of 193nm wavelength for 65nm node will require near wavelength mask features and the use of 157nm below 45nm will require sub-wavelength mask features using immersion lithography if a 4X reduction factor is maintained.

2.2 Mask Feature Aspect Ratio

Over the past decade, the fabrication process of binary photomasks has not been changed drastically. The main material used to block the light from the source has remained chrome, and chrome oxides and nitrides are used as anti-reflective layers. In particular, the thickness of the opaque layer has not scaled with feature size. Figure 2 shows a plot of the mask feature aspect ratio versus k_1 for various values of NA. An aspect ratio of 0.3 will be reached for 65nm node and could reach 0.5 for 45nm node if the reduction factor of 4X and the mask absorber thickness are kept the same.
In the case of alternating aperture in Figure 3, the aspect ratio will be around 0.9 for 65nm node and become larger than 1 for 45nm node under the same conditions.

3 Assessment of Mask Topography Effects

The mask error enhancement factor (MEEF) was originally introduced to characterize low k_1 lithography as a metric of image quality and is defined by the following equation:

$$MEEF = m\frac{\partial CDwafer}{\partial CDmask}$$

The MEEF was chosen in this study as it is a good measure of mask CD effects on printed wafer CDs. Intuitively mask topography effects will affect MEEF but this will be difficult to verify experimentally as low k_1 and mask topography effects are correlated. To understand the individual contributions, one would have to either change the mask structure or change the mask magnification. Unfortunately, both options are not very easy to implement.
In order to de-correlate the effects, simulation tools can also be used. Indeed different simulation models can reveal different imaging characteristics. Low k_1 imaging effects can be investigated using a scalar model combined with a "thin-mask" approximation. Using a vector model with the "thin-mask" approximation, low k_1 imaging and polarization effects would be combined. Finally a vector model with a "thick-mask" model would combine low k_1, polarizations and mask topography effects.
For this study, the vector / "thin-mask" and the vector / "thick-mask" models will be compared to investigate the importance of mask topography effects. To study more particularly the effect of the mask feature aspect ratio, the mask magnification will be changed using a vector / "thick mask" model.
For the rest of the paper vector models with un-polarized light will be used.
Figure 4 shows the electric field calculated at the mask level for various magnifications. The distortion of the waves as they cross the mask structure are a combination of the two main effects, the diffraction effects which will result in low k_1 issue when the diffraction orders are propagated through the optical system and the topography effect coming from the fact that the mask is a three dimensional structure.

4 Simulation Conditions

4.1 Simulation Parameters

The simulations were run using Fortis ™ Simulation Tool. This tool supports scalar and vector models with "thin-mask" and "thick-mask" options. The "thin-mask" approximation assumes that the mask is perfectly flat. The "thick-mask" approximation accounts for mask topography effects by rigorously solving Maxwell's equations at the mask level using the time-domain, finite difference techniques. The fields obtained at the mask level are propagated through the optical system to create the wafer image.
The scanner exposure conditions target 65 nm node technology using an exposure wavelength of 193nm and a numerical aperture of 0.85. The source setting was optimized for each feature size and type described in this paper.
The simulations were run for binary and phase-shifting masks. The substrate in both cases is assumed to be quartz with a refractive index of n=1.563 and k=0. The absorber is assumed to be chrome with a refractive index of n=0.84, k=1.65 and a thickness of 75nm. For the alternating phase-shifting masks, the quartz etch profiles will be assumed to be vertical with no undercut performed to balance the light between 0-degree and 180-degree openings in the mask. The light balancing will be performed by sizing the openings.
The wafer stack used for the simulations is composed of a silicon substrate (n=0.88, k=2.76), a bottom anti-reflective layer (n=1.83, k=0.34, thickness=78nm), and a resist layer (n=1.7, k=0.008, thickness=200nm). The imaging is performed in the air (n=1, k=0).

4.2 Simulation Procedure

The procedure used for the collection is described in Figure 5 and 6. The calculation of the intensity profile is performed in a two-step process (Figure 5). First, the intensity is calculated as a function of the distance along the mask and as a function of the distance inside the resist. The calculation of the intensity profile inside the resist is necessary to properly account for polarization effects since we are assuming a very large NA of 0.85. To simplify the calculation, the intensity profiles will be averaged as a function of depth inside the resist. This approximation gives a first order account of the resist effects without requiring a full resist model calculation that would be prohibitive for this study since many data points were collected.
Using the intensity calculation described in Figure 5, the MEEF is calculated as a function of the intensity threshold as shown in Figure 6. The data reported is giving the minimum MEEF for a given feature type to avoid large differences due to threshold variation between features coming from proximity effect. The value reported also represents the MEEF at the optimum intensity threshold (exposure dose) for each feature size and type.

5 Simulation Results

Figure 7 gives a plot of the MEEF as a function of magnification for various pitch values using the "thin-mask" approximation. A large change in MEEF versus feature size is observed due to low k_1 illumination but no significant change of MEEF versus magnification. From a simulation standpoint, the change in magnification should only be affected by the obliquity factor which, in this case, has a limited contribution to overall MEEF.

The result using the "thick-mask" calculation is given in Figure 8. In this case, a significant change of MEEF versus magnification is observed. This change is even amplified for smaller feature sizes thus supporting the importance of the actual mask feature size to the MEEF. This data was collected for the most practical magnifications used (4X, 5X, 6X).

In Figure 9, the MEEF was calculated as a function of a wider range of magnifications (from 4X to 10X). For the plot in Figure X, the X axis was changed to the actual feature size divided by the wavelength. A resonance effect is observed as a function of magnification with a pitch of the oscillation equal to the exposure wavelength. There is also a trend toward an increase of the MEEF for smaller magnification (or smaller mask feature sizes).

A more extreme case is reported in Figure 10 for a pitch of 115nm (57.5 nm lines and spaces feature); the following conditions were used: λ = 193nm, NA=0.9, annular illumination: 0.95-0.9. The 4X condition represents a mask feature size of 1.2 λ and an aspect ratio = 0.33. The MEEF is drastically increasing for smaller mask feature sizes, thus supporting the fact that a large portion of the MEEF is related to mask-topography effects.

This study was further extended to the case of alternating aperture phase-shifting masks. The interest of this type of masks comes from the fact that the quartz substrate is etched to create 180-degree phase-shifting regions compared to the original quartz surface. These cavities result in large mask topographies and aspect ratios close to one (see Figure 11). Previous papers have focused on light imbalance issues between etched and un-etched quartz regions caused by light scattering effects (refs). In Figure 11, we examine the effects of the mask topography on the MEEF by comparing a "thin mask" approximation and a "thick-mask" alternative at 4X and 6X magnification. The printed features in the case of the "thick-mask" calculation have been sized in order to compensate for the light imbalance between etched and un-etched quartz areas. The simulations assume that for both 4X and 6X the quartz profiles are vertical with no undercut underneath the chrome regions. A MEEF of 1.46 is reported for the "thin-mask" approximation, 2.07 for 6X magnification and 2.47 for 4X magnification thus indicating that the mask topography effects have a very significant impact on the MEEF. As expected the MEEF is low even at low k_1 for the alternating aperture phase-shifting mask but the large increase observed indicate the risk of creating a large mask topography. At 4X, the mask feature size equals 1.4 times the wavelength while the aspect ratio is 0.88.

6 Conclusions

At 4X magnification and k_1 approaching 0.25, primary mask features that will ultimately print on the wafer can be on the order of the wavelength for conventional exposure tool and could fall below wavelength for immersion lithography. At the same time, the aspect ratio of the features defined on the mask increases since the absorber thickness did not scale with the technology nodes. For alternating phase-shifting masks, the etch depth into the quartz required to create a 180 degree phase-shift has not scaled with technology nodes since it is proportional to the wavelength of exposure (which has not scaled with technology nodes). The results presented in this paper show that near wavelength and high aspect ratio mask features increase the importance of mask topography effects. Simulations were used as a mean to de-correlate the contributions of low k_1 effects versus mask topography effects. The "thin-mask" approximation results can be compared to the "thick-mask" simulation results. The effect of the feature aspect ratio can be investigated by changing the magnification factor.

Mask topography effects are shown to represent a significant part of the MEEF even for binary masks.

Acknowledgements

The authors would like to acknowledge Earnie Murphy and Randy Bennett from Brewer Science for supplying BARC optical constants and Armen Kroyan from Synopsys.

References

[1] reference on AAPSM imbalance
[2] C. Pierrat et al., IEDM 1992, pp 3.3.1-3.3.4.
more references...

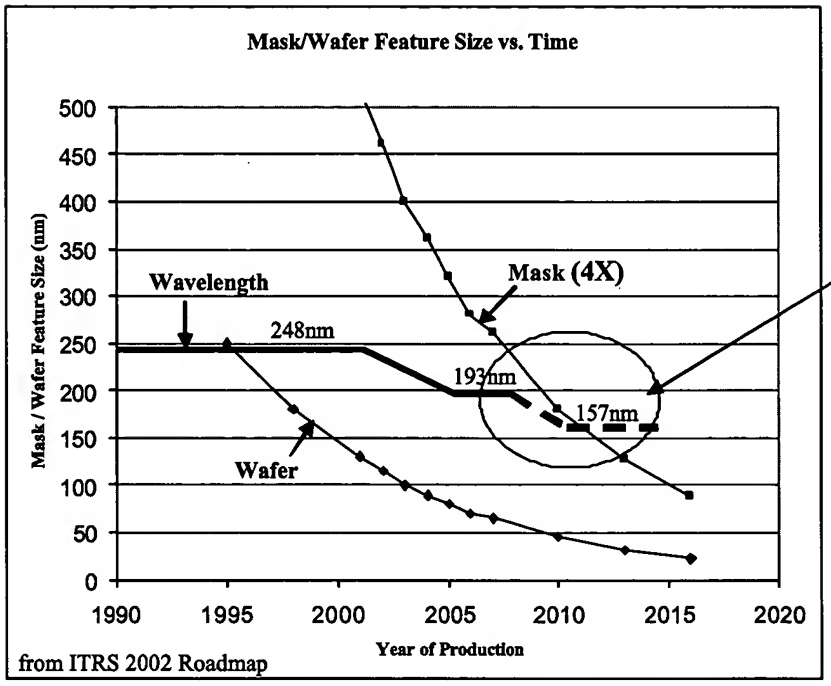

Figure 1: Mask feature size, wafer feature size, and exposure tool wavelength versus year of production. Data taken from the ITRS 2002 roadmap, wafer dimension are equal to the DRAM half pitch, mask dimensions are equal to four times the wafer dimensions.

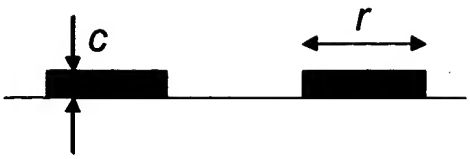

$$r = \frac{k_1 \lambda}{NA}$$

r = resolution c = chrome thickness
ar = aspect ratio m = magnification

Binary

$$ar = \frac{c}{mr} = \frac{cNA}{mk_1\lambda}$$

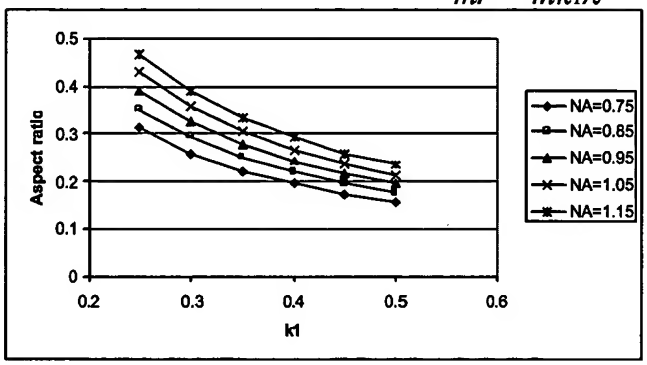

Figure 2: Mask feature aspect ratio for a binary mask. λ = 193nm, m= 4, n=1.563, c= 75nm.

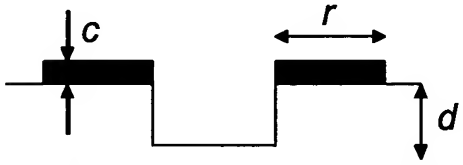

$$r = \frac{k_1 \lambda}{NA}$$

$$d = \frac{\lambda}{2(n-1)}$$

r = resolution
c = chrome thickness
m = magnification
d = quartz etch depth
ar = aspect ratio

AA PSM

$$ar = \frac{d+c}{mr} = \frac{NA(\lambda + c(2n-1))}{2mk_1(n-1)\lambda}$$

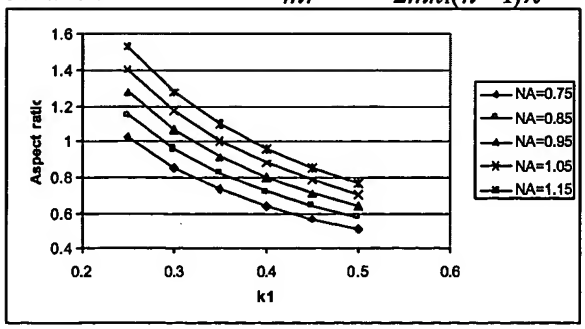

Figure 3: Mask feature aspect ratio for an alternating aperture phase-shifting mask. λ = 193nm, m= 4, n=1.563, c= 75nm.

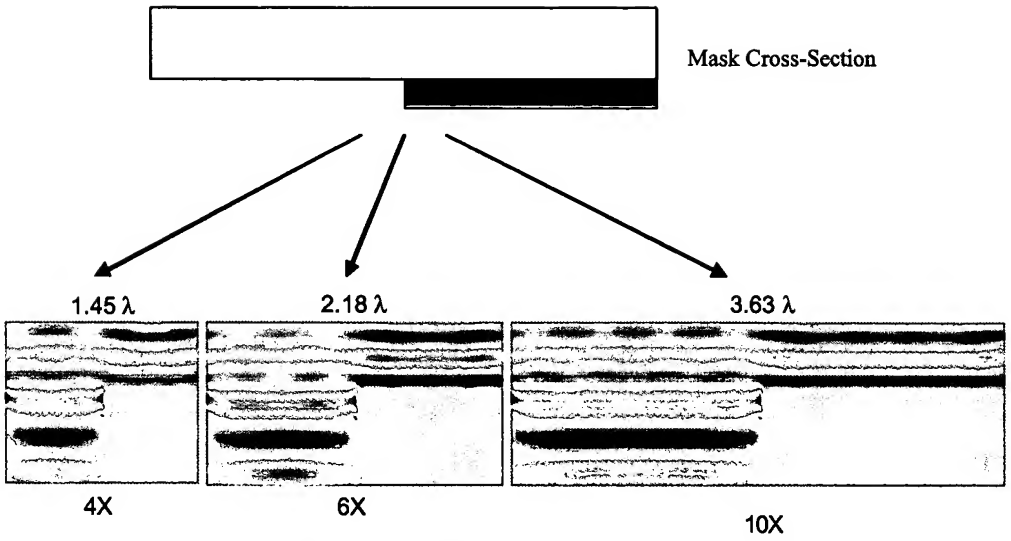

Figure 4: Example of the calculation of the electric field at the mask level for a 70nm lines and spaces pattern using a wavelength of 193nm. The calculation was performed for three different reduction factor: 4X, 6X, 10X.

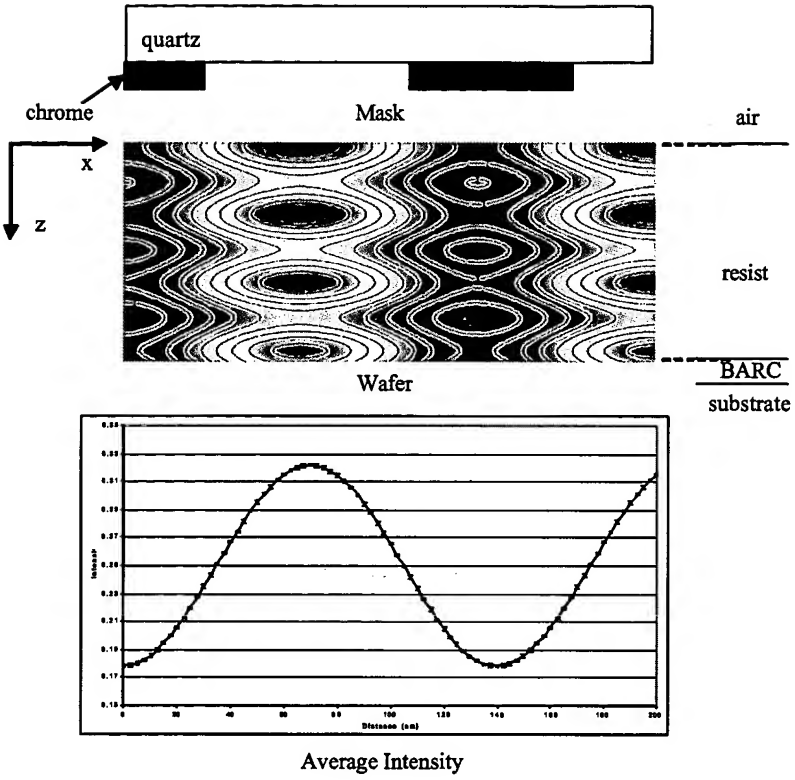

Figure 5: Simulation procedure. step1: calculate the intensity inside the resist I(x,z), step2: average the intensity over the depth inside the resist → I(x).

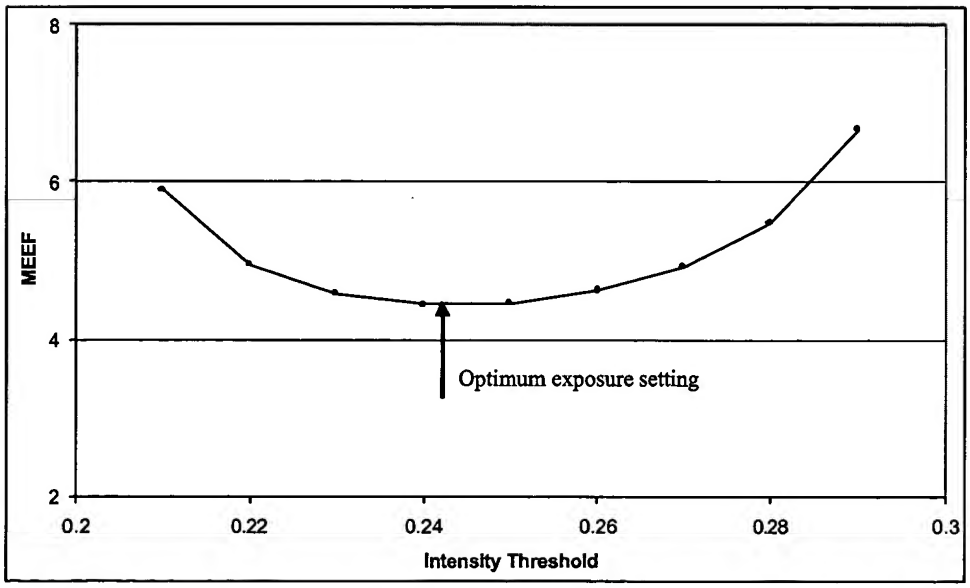

Figure 6: MEEF versus intensity threshold. The minimum MEEF obtained is used for a given feature type and size

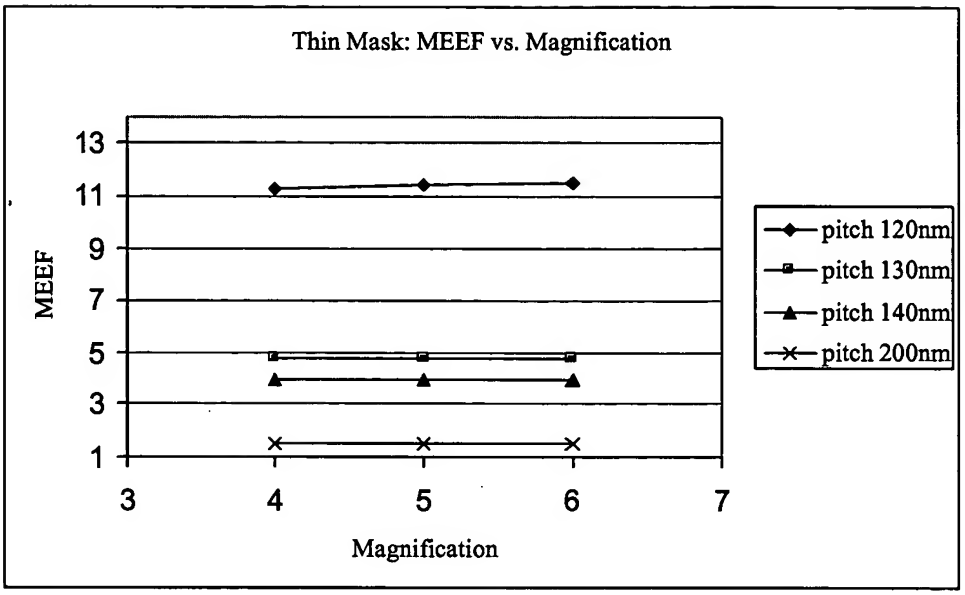

Figure 7: MEEF versus magnification for "thin-mask" approximation and equal lines and spaces patterns at various pitch: 120nm, 130nm, 140nm, 200nm.

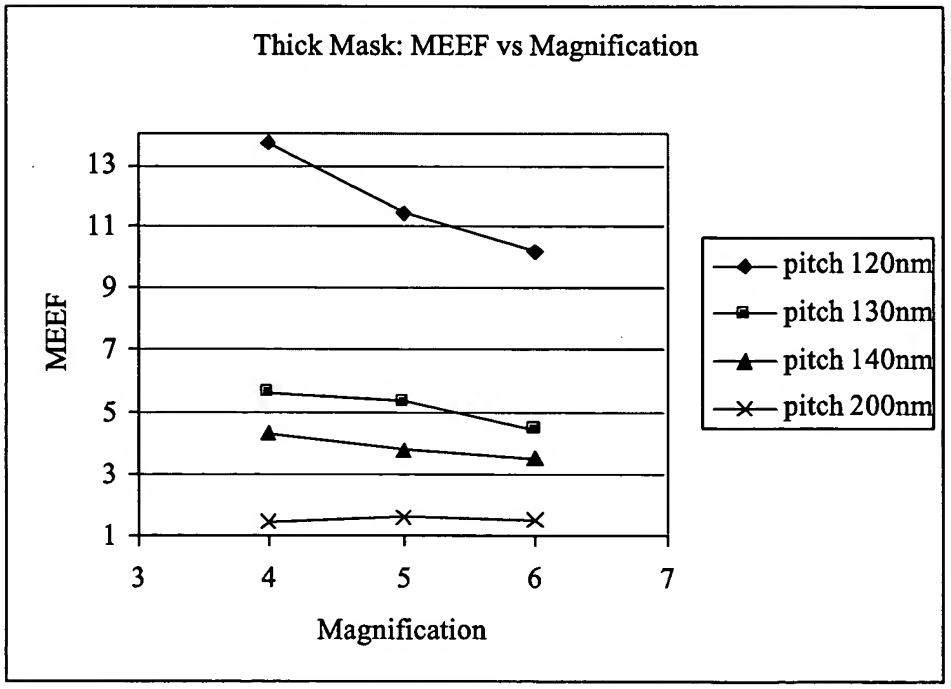

Figure 8: MEEF versus magnification for a "thick-mask" calculation and equal lines and spaces patterns at various pitch: 120nm, 130nm, 140nm, 200nm.

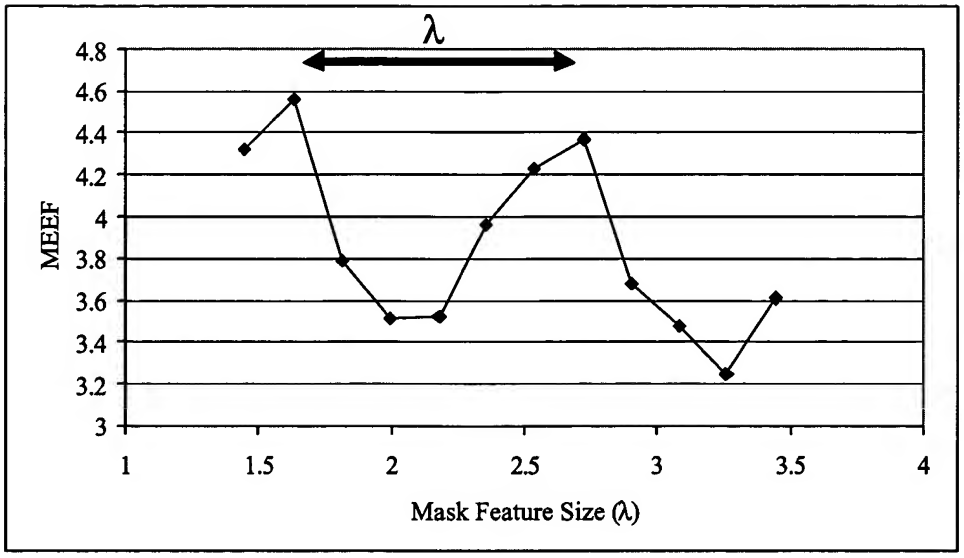

Figure 9: MEEF versus mask feature size in wavelength unit, 70nm lines and spaces

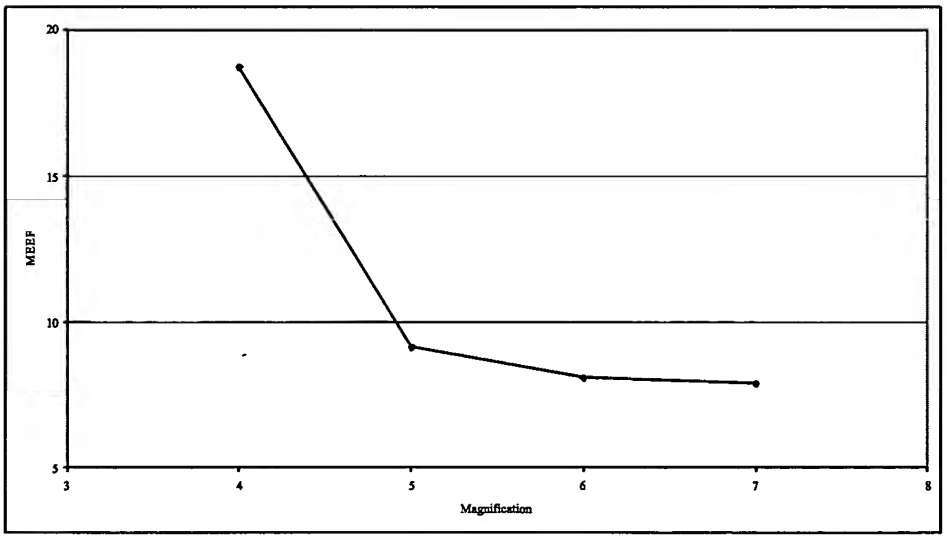

Figure 10: Pitch 115nm (57.5nm feature). Exposure setting: l = 193nm, NA=0.9, annular: 0.95-0.9
Mask feature size @4X = 1.2 l, aspect ratio = 0.33

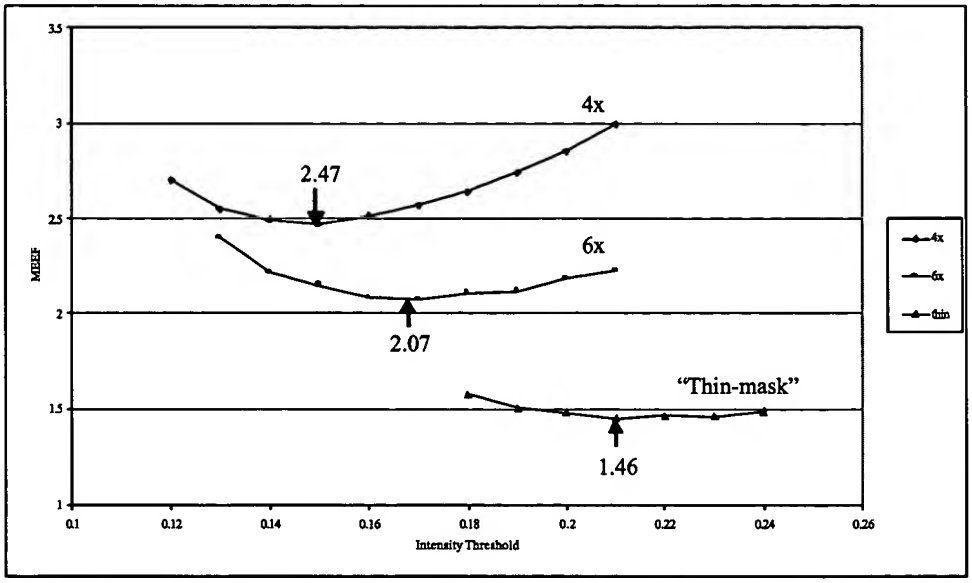

Figure 11: All dimensions at 1X, thin mask: 70nm lines and spaces, 4x: 70nm chrome lines, 60 nm 0-phase spaces, 80nm 180-phase spaces, 6x: 70nm chrome lines, 64nm 0-phase spaces, 76nm 180-phase spaces.